«Combined MRI-adaptive magneto-thermo-polychemotherapy for improved cancer treatment»

Nikolai A. Brusentsov[a], Y. A. Pirogov[b], N. V. Anisimov[b*], V. A. Polianski[c], Elena V. Verkhoglazova[b], M. R. Lichinicer[a], I. S. Golubeva[a], M. V. Gulyaev[b], M. P. Nikitin[d], T. N. Brusentsova[d], P. I. Nikitin[d]

[a]N.N. Blokhin SE Russian Cancer Research Center RAMS; [b]Research Center for Magnetic Tomography and Spectroscopy, M.V. Lomonosov Moscow State University; [c]Institute of Mechanics, Moscow State University; [d]A.M. Prokhorov General Physics Institute, RAS

Introduction:

Early detection of invasions and metastases by magnetic resonance imaging (MRI) is an important problem in detection of malignant tumors. During investigation of early stage oncogenesis and metastases by BIOSPEC BC 70/30 (Bruker), we have found that weak proton signals from small sites of pathogenic cells are neutralized by strong signals from normal tissues. To reveal the tumors by contrast-enhanced MRI, we have synthesized and tested Dextran-ferrite (DF) as the first step of our research. DF sol (DFS) was compared with some other currently used contrast agents. The second step was treating the tumors by combination of several procedures and drugs. First of all, we used Cysplatin (CP) and Melphalan (MP), which are well-known chemotherapeutic drugs for treatment of the breast, lung, ovarian and others cancer. Besides, CP's and MP's activities can be increased by combining them with DFS [1,2]. The complex treatment method that combines the magnetically controlled anticancer drugs, namely: CP and MP containing DFS; targeting them to the tumor by a gradient of permanent magnetic field (MF); heating tumor by AC MF with necrotic slime aspiration, is a well-known treatment method named as magnetohydrodynamic thermochemotherapy [1].

A more comprehensive combination of the treatment together with 3D MR-imaging as well as with quantification of magnetic agents we call as combined MRI-adaptive magneto-thermo-polychemotherapy (CAT). This paper is devoted to development of such CATs of the murine mammary Ca 755 adenocarcinoma, Lewis lungs carcinoma and B 16 melanoma based on our previous results [1-6] and new findings for MRI contrast enhancement and for quantification of magnetic agents [7] used for drug targeting and tumor hyperthermia. The goal of such research is optimization of the treatment on oncogenesis by 3D near-real-time MRI that controls CAT.

It should be noted that MRI-enhancement and targeting of the drugs in the tumor tissues was studied in [1,8,9], the DF saturation magnetization (Ms) and other physical,chemical,and biological properties were described in [4, 10-12].

Experimental:

The specific power absorption rate (SAR) of the magnetic materials was calculated from the time-temperature dependencies as the amount of power converted into the heat per gram of Fe, zeta-potential (ζ) and Gaussian/Nicomp distribution analysis of particle diameters of DF, chemotherapeutic drugs CP and MP combined with DF were studied as described in [1-6, 10-12]. DF elemental analysis was studied using plasma atomic emission spectrometry with focus on the determination of Fe as described in Ref. [6,10]. Quantification of superparamagnetic materials in DF antitumor drugs, in tumors and tissues in vitro and in vivo in mice were carried out by "BioMag" device based on non-linear magnetization of nanoparticles [7].

Dextran-ferrite was synthesized from Fe3O4 nanoparticles by covering their Dextran T10 was obtained from Sigma and the coated nanoparticles were separated magnetically. DF nanoparticles cores had diameters between 3 and 10 nm, with the hydrodynamic diameter of the coated nanoparticles being between 24 and 40 nm. Targeting of the drugs in hypodermic and skin tumors tissues were performed by SmCo5 bandages according to recommendations [8,9] or by superconducting magnet (up to 7.0 T). Results of magnetic drug targeting and time evolution of DF concentrations were monitoring by "BioMag" device [7].

We tested a 0.1% DFS in 7% dextran as magnetic resonance imaging contrast agent for CAT. For this purpose, the DF at the doses of 0.01, 0.05, and 0.08 mmol Fe/kg were injected into mice with mammary Ca 755 adenocarcinoma, Lewis lungs carcinoma and B16 melanoma. To prepare tumor-bearing animals, the Ca 755 adenocarcinoma was implanted subcutaneously into the right axillary region in 150 female C57Bl/6j mice that were 6 – 10 weeks old by injection of 106 viable tumor cells in 0.2 ml of saline, pH 7.4. The B16 melanoma was implanted similarly in 60 female C57Bl/6j mice. The Lewis lungs carcinoma was implanted intramuscular into the right femoral region in 60 female C57Bl/6j mice. The Cysplatin and Melphalan containing 40% dextran-ferrite sol were used as chemotherapeutic drugs having anti-cancer properties for CAT.

Initially, 60 mice with Ca 755 adenocarcinoma, 60 mice with Lewis lungs carcinoma and 60 mice with B16 melanoma underwent non-enhanced MRI using BIOSPEC BC 70/30 USR (Bruker), supplied by Model 1025 Small Animal Monitoring and Gating System. MR-imaging were performed with T1-weighted {500/15 [repetition time msec/echo time msec]} and T2-weighted (1,900/80) spin-echo and T2-weighted gradient-echo (GRE) (500/15) sequences. Then 0.01 – 1.0 ml DF (dose up to 12 mg Fe/kg) were injected in mice caudal vein.

Within 1-24 h the second MRI and DF-enhanced T2-weighted sequences were performed. Decrease of the signal intensity was recorded, and visual analysis was performed.

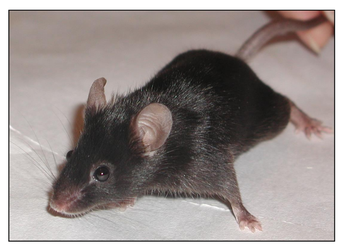

The initial CAT was performed in mice with Ca 755 separated into two sets of four groups (1,1`, 2,2` 3,3` and 4,4`) depending on mice tumor volume. In the first set (groups 1-4), the tumor volumes V reached 45 mm3 while in the second set (groups 1`-4`) V ranged from 30 to 300 mm3. Volumes were calculated as V = 0.5·(l·n2), where l was the length and n the width of the tumor. The control group 1 consisting of 20 mice was injected by 300 μl saline buffer. Ten mice from each of the 2nd, 3rd and 4th group were injected by 300 μl of CP and MP containing DF (net Fe3O4 weight: 83 mg; CP 40 μg; MP 4 μg; pH 7.4; ζ +13 mV; Ms 8.2 kA/m; SAR 260 W/g Fe). Simultaneously with the injection, a non-uniform MF was applied by SmCo5 magnetic bandages (0.2 T induction and gradient 15 mT/cm) in order to keep and concentrate the nanoparticles in the tumor tissue [1,2]. Within 30 minutes mice were placed inside a 60x200 mm air-cooled inductor with RF power for CAT, interstitial CP and MP concentrations were determined by thin layer chromatography as described earlier [1-4].

All experimental results are represented as mean ± Θ standard deviation. Statistical analysis was done as described in Ref. [13].

Results:

DF accumulation in the normal tissues successfully was visualized by MRI and quantified by "BioMag" device. The measurements have shown that DF concentration in normal tissues is 6 times higher compared with Ca 755 tissues. The DF appears to be a promising MRI-negative contrast agent for detection of early stage tubular form invasion and metastases (Fig. 1a,b), lobular form invasion and metastases (Fig. 2a,b), and mixed form invasions and metastases (Fig. 3a-d) of Ca 755. It also might be used for the oncogenesis check at CAT. Thus, experiments showed the 0.1-1.0% DFSs are MR-negative contrast agents that enhanced MR-images of the invasions and metastases. It should be emphasized that such early stages of the invasions and metastases were not detected by non-enhanced DF or magnevist. The plasma elimination half-life of DF observed by "BioMag" instruments at 0.05 mmol Fe/kg was 20 min.

From 20 min to 24 h after intravenous injection of DF, a strong MRI-enhancement of the invasions and metastases was clearly detected: in positive tumors - as clear spots on dark background (Fig. 1a, 2a, 3a-d) and in negative tumors - as inverse spots (Fig. 1b, 2b). The pathomorphological and histopathological analyses of lymph nodes and other organs revealed the presence of the invasions and metastases. DF-enhanced MRI was thus the method of choice for the differentiation of benign and malignant lymph nodes and detection of the invasions and metastases of the rest organs. Besides, with DF injection, it was possible to detect invasions and metastases of the Luis lungs carcinoma in the lungs and urine bladder in 40 mice of 50 with tumors from 120 to 300 mm3, and B 16 melanoma in the lungs and kidney in 42 mice of 50 with tumors from 150 to 300 mm3.

From 40% to 80% of DF, from 46% to 65% of CP and from 22% to 36% of MP were detected in the tumor tissues after the first injection in groups 2, 2`, 3, 3`, 4 and 4`. Accumulation of DF in tumor tissues was increased by magnetic bandage targeting and quantified by "BioMag" instruments using geometrical MRI data. Except for that, ferrite aggregates accumulated in tumor tissues were visible in Prussian blue stained sections.

After beginning of the invasions and metastases, 3 and 4 times of CATs demonstrated significant tumor responses over 36 days in groups 3, 3` and 4, 4` comparatively to control (groups 1 and 1`) and to groups 2 and 2` (Tables 1, 2). A temperature of 43 ºC for groups 2–4 and 2`–4` was reached after 6 min of CAT when the AC MF (0.88 MHz, 7.3 kA/m and 0.15 kW) was used. The temperature at the outer skin covering the tumor increased to about 45 ºC and was maintained with an accuracy of at least ±1 ºC.

CAT of ~45 mm3 Ca 755 in C57Bl/6j mice by placement of the tumors in AC MF led to hyperthermia at 46 ºC for 30 min. As the result such treatment led to tumor regression before metastases by 40%, and 280% increase of life span has been achieved (Table 1). The same treatment of ~300 mm3 metastases tumors increased the animal's life span by 200% (Table 2). Using the similar CATs for B16 melanoma of ~30 mm3 the tumor regression was 30% and of life span by 150%, for Lewis lungs carcinoma ~30 mm3 the tumor regression was 30% and of life span by 160%.

Conclusions:

Dextran-ferrite sol (DFS)-enhanced MRI was able to visualize the invasions and metastases Ca 755 in the lymph system, lungs, brain and liver which were not palpable upon physical examination and could not be visualized using the non-enhanced MRI and magnevist. Thus, DF-enhanced contrast in MRI has a considerable effect on the planning of therapy intensity. Accumulation of DF in adenocarcinoma's tissues can be significantly increased by magnetic bandage targeting and quantified by "BioMag" instruments and MRI data. The advantages of the presented combined MRI-adaptive magneto-thermo-polychemotherapy were confirmed and resulted in increased life spans of mice with Ca-755 adenocarcinoma, Lewis lungs carcinoma and B16 melanoma.

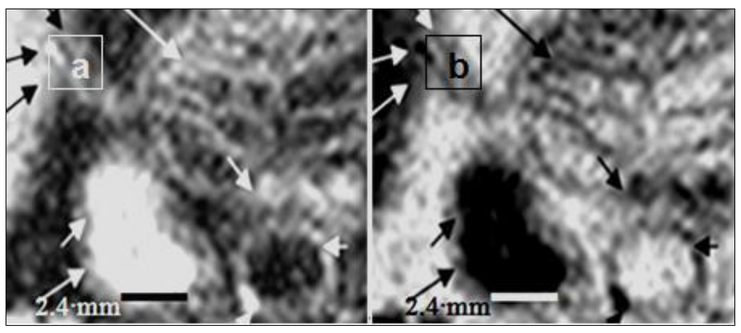

Fig. 1(a, b). MRI of tubular form Ca 755 after Dextran-ferrite sol (DFS) intravenous injections: (a) an invasion of the tumor tubs in normal muscle tissues in group 2` mice: a place of intertwisting of the tubs in a tumor in a garrot (G) and yield of the G from a tumor (black arrows); a place of an inlet, untwisting of the G and invasion of the tubs in normal tissues (major white arrows), metastases (short white arrows); (b) negative tumors - as inverse spots.

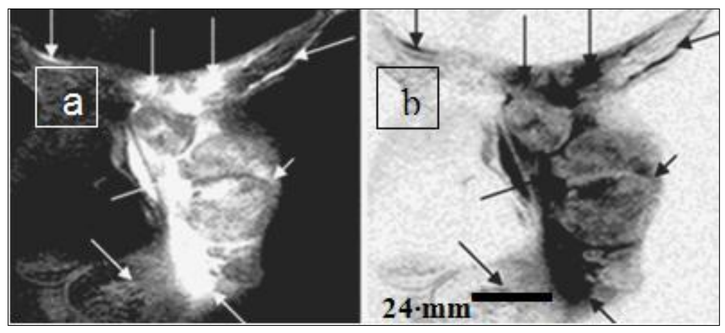

Fig. 2(a, b). MRI-monitoring of globular form Ca 755: (a) an invasion of cells in lymphatic system and other normal tissues (white arrows); (b) negative tumors - as inverse spots.

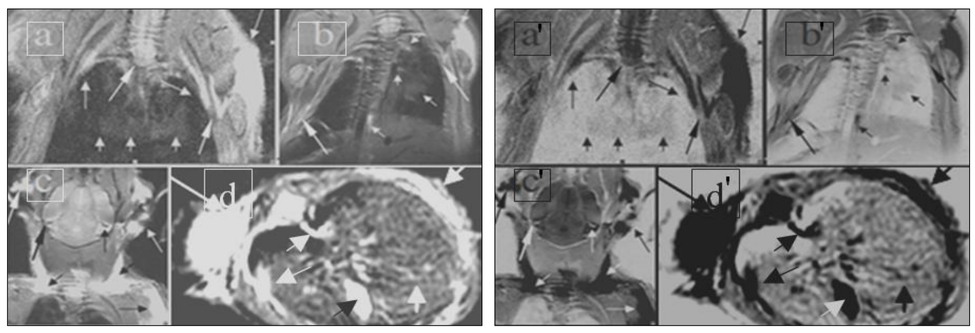

Fig. 3(a-d). MR-imiging of oncogenesis of tubular, lobular and mixed forms of the Ca 755 that was implanted similarly: (a) lobular form of tumor relapse (outside long arrow) after 3 procedures of CATs and its tubular form invasion in the lungs (long arrows) and metastases (short arrows) after 39 days after Ca 755 implantation in group 3` mice; (b) invasion in the lungs (long arrows) and metastasis in the lungs and backbone after 10 days after CATs (short arrows) in group 2` mice; (c) lobular form of tumor relapse after 6 procedures of CATs (white arrow) and it invasion in the lymphatic system and brain after 29 days after CATs (black arrows) in group 4` mice; (d) lobular form tumor relapse (outside long arrow) after 3 procedures of CATs and its tubular form invasion in the lymphatic system and liver (short white arrows), cholic bladder (black arrow) after 29 days after tumor CATs in group 4` mice.

Table 1.
CAT effect on small Ca 755 tumor (group 1-4) 36 days after the start of the treatment

Group	Number of treat-ments	Average tumor volume±SD (mm3)	Relative tumor volume	Complete regression (%)	(ILS) (%)
1	0	45.00±14.0	1.00	0	0
2	3	32.40±11.0	0.75	0	150
3	3	16.20±6.0	0.36	20	180
4	4	4.40±2.0	0.10	40	280

The increase in the life span (ILS) corresponds to the number of treatments.
Relative tumor volume = (average tumor volume of each group)/(average tumor volume of group 1).

Table 2.
CAT effect on large Ca 755 tumor (group 1`-4`) 36 days after the start of the treatment

Group	Number of treat-ments	Average tumor volume±SD (mm3)	Relative tumor volume	(ILS) (%)
1`	0	480.0±150.0	1.00	0
2`	3	290.4±91.0	0.60	94
3`	3	130.2±42.0	0.27	158
4`	4	45.0±14.0	0.09	200

The increase in the life span (ILS) corresponds to the number of treatments.

*Corresponding authors:
First author: Nikolay A.Brusentsov: +74996128037
brusentsov2005@yandex.ru
Presenting coauthor: Elena V. Verkhoglazova: +79263925672
littlena@rambler.ru

References:

[1] N.A. Brusentsov, T.N. Brusentsova, et al., J. Magn. Magn. Mat. 311 (2007) 176.
[2] N.A. Brusentsov, T.N. Brusentsova, et al., J. Magn. Magn. Mater. 293 (2005) 450.
[3] N.A. Brusentsov, L.V. Nikitin, T.N. Brusentsova, et al., J. Magn. Magn. Mater. 252 (2002) 378.
[4] N.A. Brusentsov, T.N., Brusentsova, et al., in: Biocatalytic Technology and Nanotechnology, G.E. Zaikov, (Eds) Nova Science Publishers, Inc., (2004) 59.
[5] N.A. Brusentsov, T.Yu. Glazkova, et al., Exp. Oncol. 12 (1990) 59.
[6] A.B. Syrkin, S.F. Ushkov, Ju.N. Bulychev, et al., Exp. Oncol. 12 (1990) 71.
[7] M.P. Nikitin, P.M. Vetoshko, N.A. Brusentsov, et al., J. Magn. Magn. Mat. 321, 1658 (2009).
[8] U.O. Häfeli, K. Gilmour, A. Zhou, S. Lee, M.E. Hayden, J. Magn. Magn. Mat. 311 (2007) 323.
[9] M.E. Hayden, U.O. Häfeli, J. Phys. Cond. Matter 18 (2006) S2877.
[10] T.N. Brusentsova, V.D. Kuznetsov, J. Magn. Magn. Mat. 311 (2007) 22.
[11] T.N. Brusentsova, N.A. Brusentsov, et al., J. Magn. Magn. Mater. 293 (2005) 298.
[12] N.A. Brusentsov, V.D. Kuznetsov, T.N. Brusentsova, et al., J. Magn. Magn. Mater. 272–276 (2004) 2350.
[13] O.Ju. Rebrova, The Medicine Statistic's Analysis Facts, Media Sphere, Moscow, 2002.